JCI insight

Extracellular CIRP induces macrophage endotoxin tolerance through IL-6R-mediated STAT3 activation

Mian Zhou, … , Gaifeng Ma, Ping Wang

JCI Insight. 2020. https://doi.org/10.1172/jci.insight.133715.

Research In-Press Preview **Immunology** **Inflammation**

Extracellular cold-inducible RNA-binding protein (eCIRP) is a damage-associated molecular pattern, whose effect on macrophages is not entirely elucidated. Here we identified that eCIRP promotes macrophage endotoxin tolerance. Septic mice had higher serum levels of eCIRP; this was associated with a reduced ex vivo immune response of their splenocytes to LPS. Pretreatment of macrophages with recombinant murine (rm) CIRP resulted in a tolerance to LPS stimulation as demonstrated by a significant reduction of TNF-α production. We found that eCIRP increased phosphorylation of STAT3 (pSTAT3) in macrophages. A STAT3 inhibitor, Stattic, rescued macrophages from rmCIRP-induced tolerance by restoring the release of TNF-α in response to LPS stimulation. We discovered strong binding affinity between eCIRP and IL-6R as revealed by Biacore, FRET, and their co-localization in macrophages by immunostaining assays. Blockade of IL-6R with its neutralizing Ab significantly inhibited eCIRP-induced pSTAT3 and restored LPS-stimulated TNF-α release in macrophages. Incubation of macrophages with rmCIRP skewed them towards a M2 phenotype, while treatment with anti-IL-6R Ab prevented rmCIRP-induced M2 polarization. Thus, we have demonstrated that eCIRP activates pSTAT3 via a novel receptor IL-6R to promote macrophage endotoxin tolerance. Targeting eCIRP appears to be a new therapeutic option to correct immune-tolerance in sepsis.

Extracellular CIRP induces macrophage endotoxin tolerance through IL-6R-mediated STAT3 activation

Mian Zhou, MD[1]; Monowar Aziz, PhD[1,2]; Naomi-Liza Denning, MD[1,2,3]; Hao-Ting Yen, MS[1]; Gaifeng Ma, MD[1]; and Ping Wang, MD[1,2,3*]

[1]Center for Immunology and Inflammation, The Feinstein Institutes for Medical Research, Manhasset, New York.
[2]Elmezzi Graduate School of Molecular Medicine, Manhasset, New York.
[3]Department of Surgery, Donald and Barbara Zucker School of Medicine at Hofstra/Northwell, Manhasset, New York.

Running title: eCIRP-IL-6R-STAT3 pathway and macrophage tolerance.

Key words: eCIRP; macrophage; endotoxin; immune tolerance; IL-6R; STAT3

***Address for all correspondence:**

Ping Wang, MD
Professor and Chief Scientific Officer
The Feinstein Institutes for Medical Research
Vice Chairman for Research
Department of Surgery, Zucker School of Medicine at Hofstra/Northwell
350 Community Dr., Manhasset, NY 11030
Tel: (516) 562-3411
Fax: (516) 562-2396
E-mail: pwang@northwell.edu

Abstract

Extracellular cold-inducible RNA-binding protein (eCIRP) is a damage-associated molecular pattern, whose effect on macrophages is not entirely elucidated. Here we identified that eCIRP promotes macrophage endotoxin tolerance. Septic mice had higher serum levels of eCIRP; this was associated with a reduced ex vivo immune response of their splenocytes to LPS. Pretreatment of macrophages with recombinant murine (rm) CIRP resulted in a tolerance to LPS stimulation as demonstrated by a significant reduction of TNF-α production. We found that eCIRP increased phosphorylation of STAT3 (pSTAT3) in macrophages. A STAT3 inhibitor, Stattic, rescued macrophages from rmCIRP-induced tolerance by restoring the release of TNF-α in response to LPS stimulation. We discovered strong binding affinity between eCIRP and IL-6R as revealed by Biacore, FRET, and their co-localization in macrophages by immunostaining assays. Blockade of IL-6R with its neutralizing Ab significantly inhibited eCIRP-induced pSTAT3 and restored LPS-stimulated TNF-α release in macrophages. Incubation of macrophages with rmCIRP skewed them towards a M2 phenotype, while treatment with anti-IL-6R Ab prevented rmCIRP-induced M2 polarization. Thus, we have demonstrated that eCIRP activates pSTAT3 via a novel receptor IL-6R to promote macrophage endotoxin tolerance. Targeting eCIRP appears to be a new therapeutic option to correct immune-tolerance in sepsis.

Introduction

Macrophage "endotoxin tolerance" is defined as a state of lipopolysaccharides (LPS) hypo-responsiveness, in which macrophages pre-exposed to endotoxin produce decreased levels of inflammatory mediators upon re-stimulation with LPS (1, 2). Endotoxin tolerance serves as an important regulatory mechanism to control excessive inflammation. However, prolonged immune tolerance allows the development of secondary infections, increasing morbidity and mortality from sepsis, trauma and ischemia/reperfusion (I/R) injuries (3, 4).

Tolerant macrophages produce lower levels of the inflammatory cytokine tumor necrosis factor-α (TNF-α) and increased levels of the anti-inflammatory cytokines IL-10 and transforming growth factor β (TGFβ) as compared to their non-sensitized counterparts (1, 2, 5-8). Macrophage endotoxin tolerance has been associated with decreased Toll-like receptor 4-myeloid differentiation factor 88 (TLR4-MyD88) complex formation (9), defects in the activation of mitogen-activated protein kinases (MAPKs) and NF-kB (1, 10), and the upregulation of negative regulators like IL-1R associated kinase-M (IRAK-M) (11), ST2 (12), and suppressor of cytokine signaling 1 (SOCS1) (13).

M2 macrophages, like endotoxin tolerant macrophages, also produce less pro-inflammatory cytokines (e.g. IL-12, TNF-α) and more anti-inflammatory cytokines (e.g. IL-10) (1, 14, 15). The signal transducer and activator of transcription 3 (STAT3) pathway plays a pivotal role in both macrophage M2 polarization and macrophage immune tolerance (16, 17). IL-6, a pleiotropic cytokine, is mainly produced in macrophages and lymphocytes (18). IL-6 binds to the IL-6 receptor (IL-6R) which is composed of two membrane associated proteins: an 80 kDa α unit for binding IL-6 and 130 kDa β unit (also known as gp130) for downstream signal transduction to activate Janus kinase (JAK) and the phosphorylation of STAT3 (18). STAT3

activation consequently regulates inflammatory cascades and also can promote M2 polarization (16, 19, 20). Since M2 macrophages resemble endotoxin tolerant macrophages, the involvement of IL-6R-STAT3 signaling in macrophage endotoxin tolerance is logical.

The mechanisms of macrophage endotoxin tolerance have mainly been elucidated in LPS-TLR4-mediated endotoxin tolerance or homotolerance. However, endotoxin tolerance can also develop upon pre-exposure of macrophages to TLR2 ligands (e.g., lipoteichoic acid), a phenomenon known as cross-tolerance, (21-23) or from chronic exposure to TNF-α and IL-1β (21). Although damage-associated molecular pattern (DAMP) has been shown to induce tolerance in macrophages (24), the concept and mechanism of DAMP-mediated endotoxin tolerance is less well described.

Cold-inducible RNA-binding protein (CIRP) is an 18-kDa RNA chaperone that regulates the translation of stress response genes intracellularly (25). CIRP is expressed in numerous cell types including macrophages, neutrophils, and epithelial and endothelial cells [reviewed in (26)]. Hypoxia, sepsis, and hemorrhagic shock (HS) can induce the release of CIRP into the extracellular space (26, 27). CIRP is released from macrophages and other cells actively by lysosomal exocytosis pathway, and passively by cellular necrosis (26, 27). Extracellular CIRP (eCIRP) is a new DAMP that fuels inflammation and organ injury in sepsis, HS, and organ I/R (26, 27). Increased serum levels of eCIRP is correlated with sepsis severity in patients (27, 28). In macrophages, eCIRP induces inflammation by binding to its receptor TLR4 (26). However, akin to other DAMPs (29, 30), eCIRP may have numerous receptor(s) other than TLR4 to stimulate immune responses. eCIRP-mediated inflammation through TLR4 has been well studied, while its role in promoting macrophages immune tolerance has not been explored. We

therefore aimed to study the effects of eCIRP on macrophage endotoxin tolerance and define potential mechanisms for this phenomenon.

We found that pre-treatment of macrophages with recombinant CIRP significantly decreased their responsiveness to subsequent LPS stimulation. We revealed that eCIRP-induced macrophage immune tolerance was associated with the activation of STAT3. IL-6R and JAK are often utilized to initiate STAT3 activation (18). We identified high binding affinity between eCIRP and IL-6R and demonstrated that this binding resulted in STAT3 activation, promoting immune tolerance in macrophages. Thus, we have identified a new mechanism for eCIRP's deleterious effects in inflammation – the induction of macrophage endotoxin tolerance through IL-6R-mediated STAT3 activation. This novel finding identifies a new therapeutic target to prevent sepsis-mediated immunosuppression.

Results

eCIRP promotes macrophage endotoxin tolerance.

Murine polymicrobial sepsis is bimodal with an early hyperdynamic phase (2-10 h after CLP) characterized by an overwhelming inflammatory response, followed by a late hypodynamic phase (20 h after CLP) resulting in immunosuppression or tolerance (31-34). We assessed serum levels of eCIRP in septic mice 72 h after CLP and correlated the results with the amount of TNF-α produced by splenocytes isolated from the spleens of the same mice after ex vivo LPS stimulation. Interestingly, we found that the higher serum levels of eCIRP after CLP correlated with decreased TNF-α production by splenocytes after ex vivo LPS stimulation **(Figure 1A)**. Correspondingly, splenocytes isolated from mice with lower serum levels of eCIRP produced higher levels of TNF-α upon stimulation with LPS **(Figure 1A)**. We also assessed their serum levels of TNF-α and found parallel to their serum levels of eCIRP **(Figure 1B)**.

We performed an in vitro experiment by pre-treating peritoneal macrophages isolated from healthy mice with either PBS or recombinant murine (rm) CIRP for 24 h, and then we re-stimulated these cells with LPS for 5 h. We found that peritoneal macrophages pre-treated with rmCIRP produced significantly decreased levels of TNF-α and IL-6 by 82% and 90%, respectively, in the culture supernatants compared to cells untreated with rmCIRP **(Figure 1C, D)**. A similar finding was obtained in the macrophage cell-line RAW264.7, in which pre-treatment with various doses of rmCIRP resulted in significantly decreased production of TNF-α and IL-6 in the supernatants in a dose-dependent manner, compared to pre-rmCIRP untreated controls after stimulation with a fixed dose of LPS **(Figure 1E, F).** Next, in an in vivo study, we injected mice with rmCIRP *i.p.,* isolated peritoneal macrophages 24 h later and stimulated with LPS ex vivo for 5 h. We found that the peritoneal macrophages isolated from rmCIRP-injected mice produced significantly decreased levels of IL-6 by 74% and 67% at 25 and 50 ng/ml of LPS

stimulation, respectively, compared to macrophages isolated from saline-injected mice **(Figure 1G)**. Collectively, the results of these in vitro, ex vivo, and in vivo studies confirm eCIRP's ability to induce immune tolerance in macrophages.

STAT3 is activated in eCIRP-treated macrophages.

STAT3 has been shown to play an important role in macrophage immune tolerance (17). In order to explore the direct effect of eCIRP on STAT3, we assessed STAT3 activation/phosphorylation in RAW264.7 macrophages after treatment with rmCIRP. We found that the amount of phosphorylated STAT3 (pSTAT3) was significantly increased in RAW264.7 macrophages after treatment with rmCIRP in a time- and dose-dependent manner compared to PBS-treated macrophages **(Figure 2A, B)**. Similarly, in splenocytes isolated from a normal healthy mouse, treatment with rmCIRP significantly increased the activation of STAT3 in a time-dependent manner **(Figure 2C)**. Since RAW264.7 cells robustly increase their inflammatory markers upon treatment with TLR agonists, we choose to assess STAT3 activity at a comparatively earlier time point (≤5 h) after rmCIRP stimulation than in primary mouse splenocytes **(Figure 2A-C)**. However, we also observed the increase of pSTAT3 in splenocytes after treatment with rmCIRP for 5 h **(Supplemental Figure 1)**. We further injected mice with rmCIRP *i.p.* and assessed STAT3 activation in the peritoneal macrophages 24 h later. There was increased activation of STAT3 in the macrophages isolated from rmCIRP-treated mice as compared to saline-treated mice **(Figure 2D)**. Collectively, this data demonstrates that eCIRP serves as a novel inducer of STAT3 activation in macrophages.

Inhibiting STAT3 reverses eCIRP-induced macrophage endotoxin tolerance.

Stattic, a selective inhibitor of STAT3 prevents activation, dimerization, and nuclear translocation of STAT3 by interacting with the SH2 domain. We found that pre-treatment of RAW264.7 cells with rmCIRP induced endotoxin tolerance. This was evidenced by significantly decreased levels of TNF-α and IL-6, 80% and 58%, respectively, in the supernatants of pre-treated LPS-stimulated cells as compared to untreated LPS-stimulated controls **(Figure 3A, B)**. Treating macrophages with rmCIRP and Stattic mitigated the development of endotoxin tolerance **(Figure 3A, B)**. Thus, eCIRP-induced macrophage endotoxin tolerance can be partially corrected by the inhibition of STAT3.

Discovery of IL-6R as a novel biologically active receptor of eCIRP.

IL-6R signaling promotes STAT3 activation (18). We therefore aimed to determine whether or not eCIRP has any interaction with IL-6R. We found a dramatic increase in the expression of IL-6R on the surface of RAW264.7 cells following treatment with rmCIRP at both 24 and 48 h compared to PBS-treated cells **(Figure 4A)**. To study the direct interaction between eCIRP and IL-6R, we performed a surface plasmon resonance (SPR), also known as Biacore assay, which demonstrated a strong binding between recombinant human (rh) CIRP and rhIL-6R with a K_D of 9.8×10^{-8} M **(Figure 4B).** The binding of eCIRP and IL-6R was even more stronger than the binding between IL-6R and its putative ligand IL-6, whose K_D was shown to be higher (35) than the K_D of eCIRP's binding to IL-6R. Of note, murine and human CIRP exhibit 95% amino acid sequence homology. We next performed an immunofluorescence study to confirm the co-localization of eCIRP and IL-6R in macrophages after rmCIRP stimulation. It clearly demonstrated the co-localization of rmCIRP and IL-6R, as indicated by the merged (yellow) image (**Figure 4C)**. Conversely, rmCIRP did not co-localize with a negative control, the

macrophage pan marker CD11b (**Figure 4C).** We also performed FRET analysis to quantitatively determine rmCIRP's association with IL-6R. FRET analysis revealed a clear association between rmCIRP and IL-6R with an increase in FRET units of 17-fold compared to rmCIRP's interaction with negative control CD11b **(Figure 4D).** These findings reveal that eCIRP is a novel ligand of IL-6R.

Blocking IL-6R by its neutralizing Ab attenuates eCIRP-induced STAT3 activation and corrects macrophage endotoxin tolerance.

After we confirmed eCIRP is a novel ligand of IL-6R **(Figure 4)**, we aimed to further study the biological significance of the eCIRP-IL-6R interaction on STAT3 activation and macrophage endotoxin tolerance. To accomplish this, we pre-treated primary murine splenocytes with anti-IL-6R neutralizing Ab or isotype IgG and, after stimulating these cells with rmCIRP, we assessed intracellular STAT3 activity. We found that splenocytes pre-treated with anti-IL-6R Ab showed significant decreases in the frequencies (%) of pSTAT3 positive macrophages ($F4/80^{+}$) by 68% compared to isotype IgG-treated spelenocytes after rmCIRP stimulation **(Figure 5A)**. Similarly, the murine primary peritoneal macrophages pre-treated with anti-IL-6R Ab showed significant decreases in the levels of pSTAT3 compared to isotype IgG-treated macrophages after stimulation with rmCIRP for 24 h **(Figure 5B)**. Interestingly, although TLR4 serves as one of the receptors of eCIRP, the effects of rmCIRP on STAT3 activation in wild-type (WT) macrophages treated with anti-TLR4 neutralizing Ab or in $TLR4^{-/-}$ macrophages treated with IL-6R Ab did not show significant difference compared to either isotype IgG-treated or WT macrophages **(Supplemental Figure 2A, B)**. Furthermore, immunostaining studies showed that the binding of rmCIRP to IL-6Rα was not impaired in $TLR4^{-/-}$ macrophages **(Supplemental**

Figure 2C). Finally, we studied the effect of anti-IL-6R Ab on eCIRP-induced macrophage endotoxin tolerance. We found that the peritoneal macrophages of anti-IL-6R Ab treatment partially corrected the endotoxin tolerance by 63% compared to the peritoneal macrophages of isotype IgG-treated condition **(Figure 5C)**. These results suggest that blocking IL-6R inhibits eCIRP-induced STAT3 activation and reverses endotoxin tolerance.

We further confirmed the critical role of IL-6R on macrophage endotoxin tolerance by using positive and negative controls. We treated macrophages with recombinant mouse (rm) IL-6 which served as a positive control and with siRNA of murine IL-6R to inhibit IL-6R expression to serve as a negative control. We found that treating macrophages with rmIL-6 significantly increased pSTAT3 in a time-dependent manner compared to PBS-treated cells **(Figure 5D)**. We also found that the macrophages pre-treated with rmIL-6 demonstrated endotoxin tolerance **(Figure 5E)**. Interestingly, we noticed more potent LPS tolerance in rmCIRP-pre-treated macrophages as compared to rmIL-6-pre-treated macrophages **(Figure 5E),** which could be due to the possible interaction of eCIRP with its other receptor(s) like TLR4 (27). We transfected macrophages with siRNA for IL-6R, which resulted in significant inhibition of the expression of IL-6R at protein levels **(Supplemental Fig 3)**. Macrophages with decreased expression of IL-6R failed to exhibit substantial endotoxin tolerance, while the macrophages treated with negative control siRNA still demonstrated endotoxin tolerance after pre-treatment with rmCIRP **(Figure 5F, G)**. These data clearly demonstrate the pivotal role of eCIRP-IL-6R axis in macrophage endotoxin tolerance.

eCIRP polarizes macrophages towards M2 phenotype through IL-6R.

Since the characteristic features of M2 macrophages resemble that of endotoxin tolerant macrophages, we assessed the M2 markers in rmCIRP-treated RAW264.7 cells at various time-points (5, 24, and 48 h) of rmCIRP treatment. We found that the expression of arginase-1 (Arg-1) mRNA was dramatically increased at the later time points (24 and 48 h) of rmCIRP stimulation compared to PBS-treated cells **(Figure 6A)**. We also found that treatment of RAW264.7 cells with rmCIRP increased the expression of M2 markers Arg-1 and CD206 in a dose-dependent manner **(Figure 6B, C)**. Morphological change serve as one of the markers of macrophage polarization (36). The morphology of RAW264.7 cells was changed to a M2 phenotype as demonstrated by their larger size than M1 macrophages **(Supplemental Figure 4A)**. These data were consistent with the finding of significantly increased frequencies (%) of CD206 in the peritoneal macrophages isolated from in vivo rmCIRP (*i.p.*) injected mice **(Supplemental Figure 4B)**. Conversely, if the IL-6R in RAW264.7 cells was blocked with anti-IL-6R Ab treatment, the expression of Arg-1 mRNA and the frequencies (%) of CD206 were significantly decreased by 43% and 22%, respectively, compared to isotype IgG treated cells following stimulation with rmCIRP **(Figure 6D, E)**. Taken together, eCIRP released during inflammation recognizes its novel receptor IL-6R to activate STAT3, which leads to macrophage endotoxin tolerance and macrophage M2 polarization. Blocking IL-6R with neutralizing antibody abrogates these phenomenon in macrophages **(Figure 7)**.

Discussion

In sepsis, the overwhelming inflammatory response is accompanied by the subsequent development of immune tolerance which results in additional detrimental outcomes (32). In the current study, we discovered a new receptor of eCIRP, IL-6R, which played a critical role in macrophage tolerance. We found a dramatic increase in the expression of IL-6R in rmCIRP-treated macrophages. On the other hand, the macrophage expression of IL-10R, which also plays a pivotal role in immune regulation, was markedly lower than the expression of IL-6R at both basal and rmCIRP-treated conditions **(Supplemental Figure 5)**. We further verified the biological function of the eCIRP-IL-6R interaction via STAT3 activation and the development of macrophage endotoxin tolerance. Interestingly, we noticed that blockade of IL-6R with its neutralizing Ab dramatically reduced pSTAT3 in rmCIRP-treated macrophages and improved immune responsiveness following LPS stimulation. In addition, we also found that the inhibition of IL-6R prevented eCIRP-induced macrophage M2 polarization, thus strongly implicating the IL-6R-STAT3 axis for eCIRP-mediated immune regulation. In the present study, although we did not focus how eCIRP increased the expression of IL-6R, we speculate that increased expression of IL-6R in macrophages after eCIRP stimulation could be through TLR4, as well as possibly by positive feedback loop after binding to the IL-6R.

The scientific premise of this study initiated with our finding that septic mice with higher serum levels of eCIRP also demonstrated immune tolerance, as they contained splenocytes that produced decreased levels of the inflammatory cytokine TNF-α after ex vivo treatment with endotoxin. We have showed direct evidence of eCIRP-mediated macrophage endotoxin tolerance in primary macrophages, as well as in the RAW264.7 cell-line. In both cell populations, we observed decreased levels of TNF-α and IL-6 after treatment with LPS in cells that had been pre-

treated with rmCIRP. These findings were consistent with the in vivo results; peritoneal macrophages from rmCIRP-injected mice produced decreased levels of IL-6 after treatment with LPS ex vivo.

In addition to endotoxin tolerance, polarization of macrophages to the M2 phenotype may contribute to immune modulation (37). It has previously been shown that the M1 to M2 macrophage reprogramming that develops during LPS tolerance resembles the pathological anti-inflammatory response to sepsis (38). Here, we confirmed that the macrophages treated with rmCIRP rapidly increased the expression of the M2 markers Arg-1 and CD206, indicating these cells were skewed towards an M2 phenotype.

Our next focus was to identify a mechanism by which eCIRP induced endotoxin tolerance in macrophages. Previously, it has been shown that STAT3 plays a pivotal role in suppressing various TLRs-mediated signal transduction in phagocytes (39, 40). Macrophages, neutrophils, and dendritic cells (DCs) that are deficient in STAT3 produce elevated levels of pro-inflammatory cytokines (TNF-α, IL-6, IL-12, and IFN-γ) through the TLR4 pathway (39, 40). IL-10, an anti-inflammatory cytokine, also regulates immune response. The anti-inflammatory function of IL-10 is mediated through the activation of STAT3 (41). Therefore, STAT3 was a viable candidate to study eCIRP-mediated immune tolerance in macrophages. NF-κB, MAPK, and IRF3 signaling cascades mainly promote pro-inflammatory genes transcription. By contrast, STAT3 has been found to induce expression of transcriptional repressors and co-repressors that inhibit NF-κB gene reporters (42), suggesting an indirect mechanism by which STAT3 restrains pro-inflammatory gene transcription.

Immune tolerance is a common phenomenon in cancer; inhibiting immune tolerance via immunotherapy improves outcomes in cancer therapy (43). It has been shown that STAT3-

defficient macrophages exhibit a constitutively activated phenotype and are more prone to produce inflammatory mediators such as IL-6, IL-12, RANTES, MIP-1α, MIP-1β, MIP-2 in response to LPS stimulation, suggesting STAT3 signaling as a negative regulatory pathway in these cells (44). Several studies have shown the pro-oncogenic role of CIRP. CIRP was found to be overexpressed in prostate, breast, liver, and colon cancers (45-48). Downregulation of CIRP enhanced chemosensitivity and impaired survival of prostate cancer cells (45). The interaction between CIRP and STAT3 has been implicated in liver cancer, in which the tumor bearing wild-type mice had a higher level of pSTAT3 than $CIRP^{-/-}$ mice (48). Interestingly, in our study we found dramatic upregulation of pSTAT3 in macrophages and splenocytes after treatment with rmCIRP. Splenocytes contain mixed cell populations such as macrophages, T and B cells. We found that macrophages of the spleen were more responsive to eCIRP for the induction of STAT3 phosphorylation than other cell types **(Supplemental Figure 6)**. We further determined the impact of STAT3 signaling on eCIRP-induced macrophage endotoxin tolerance by using an inhibitor of STAT3 Stattic, which mitigated rmCIRP-induced macrophage endotoxin tolerance. We have shown that, under in vitro conditions, blocking STAT3 by Stattic partially corrected immune tolerance in eCIRP-induced RAW264.7 cells. The degree of rescue likely depends on factors such as optimal time points, which we may not have captured. Several factors that influence RAW264.7 cells' activity including confluency, passage number, and cell numbers might influence the optimum conditions for blocking STAT3 to reverse eCIRP-induced immune tolerance. In addition, aside from STAT3-mediated tolerance, several other pathways/molecules including TLR4/MyD88's negative regulators IRAK-M, ST2, SOCS1 and SOCS3 are involved in tolerance induction in macrophages. eCIRP has been previously shown to recognize the TLR4/MD2 complex (27). Therefore, future studies on the involvement of these molecules will

provide additional insight into the mechanism of eCIRP-mediated induction of immune tolerance in macrophages.

We next sought to determine how eCIRP induces STAT3 activation in macrophages. STAT3 is upregulated via the JAK family of proteins associated with putative receptors like cytokine receptors, G-protein coupled receptors, growth factor receptor, and tyrosine kinase receptors, which are recognized by a large number of cytokines (IL-6, IL-10, IFNs) and growth factors (EGF, G-CSF, GM-CSF, VEGF) (49). Here, we identified IL-6R to serve as a novel receptor of eCIRP to activate downstream mediator STAT3, which in turn led to macrophage endotoxin tolerance.

Septic patients who survive the acute stage of sepsis often develop a chronic critical illness associated with immunosuppression leading to high morbidity and mortality (50). In humans, increased levels of eCIRP in the serum have been shown to correlate with sepsis severity (27, 28). We discovered a novel link between eCIRP and IL-6R in murine macrophages to promote eCIRP-induced macrophage endotoxin tolerance; this provides a strong premise for studying eCIRP's role in immune tolerance in septic patients. We showed that anti-IL-6R Ab reversed eCIRP-induced macrophage endotoxin tolerance. Since strategies with neutralizing Ab targeting a signaling pathway might exhibit off target effects, future discoveries of a small peptide targeting the eCIRP-IL-6R interaction could be helpful to counter eCIRP-induced immune tolerance in macrophages to safeguard patients from secondary infection. We used in vitro, in vivo, and ex vivo approaches to study eCIRP's role in macrophage endotoxin tolerance, which opened up a new direction to validate our findings in various pre-clinical models susceptible to the development of immune tolerance resulting in secondary infections.

Materials and Methods

Reagents and antibodies

Reagents and culture mediums for cell cultures were purchased from Sigma-Aldrich (St. Louis, MO) and Thermo Fisher Scientific (Waltham, MA). Goat anti-mouse IL-6R polyclonal neutrilizing Ab (catalog no.: AF1830) and normal goat IgG (catalog no.: AB-108-C) were purchased from R&D systems (Minneapolis, MN). Anti-mouse TLR4/MD2 neutrilizing Ab (clone: MTS510, catalog no.: 117608) were from Biolegend (San Diego, CA). STAT3 inhibitor (Stattic) was purchased from Santa Cruz (Santa Cruz, CA) and recombinant mouse (rm) IL-6 was from R&D Systems, Inc. (Minneapolis, MN). Abs for flow cytometry: PE anti-mouse pSTAT3 (Tyr705, clone: 13A3-1; catalog no.: 651004), PE/Cy7 and pacific blue anti-mouse F4/80 (clone: BM8; catalog no.: 123114 and 123124) and PE/Cy7 anti-mouse IL-6R (clone: D7715A7; catalog no.: 115814) were from Biolegend. Abs for western blotting: anti-mouse pSTAT3 (Tyr705; catalog no.: 9131) and total STAT3 (catalog no.: 9139) were from Cell Signaling Technologies (Danvers, MA). β-actin Ab (clone: AC-15, catalog no.: A5441) was from Sigma-Aldrich. Infrared dye labeled secondary Abs were from Li-Cor Biosciences (Lincoln, NE). Abs for immunocytochemistry staining and FRET analysis: rabbit anti-mouse CIRP Ab (catalog no.: 10209-2-AP) was from ProteinTech (Rosemont, IL). Goat anti-mouse CD11b Ab (catalog no.: MBS420973) was from MyBiosource (San Diego, CA). Fluorescent labeled secondary Ab Cy3-conjugated donkey anti-rabbit IgG (catalog no.: 711-166-152) and Cy5-conjugated donkey anti-goat IgG (catalog no.: 705-175-147) were from Jackson immunoResearch Lab (West Grove, PA).

Experimental animals and sepsis induction

Male C57BL/6 mice (9-12 weeks-old) were purchased from Charles River Laboratories (Wilmington, MA). Animals were housed in a temperature-controlled room with a 12 h light-dark cycle and fed a standard Purina rodent chow diet. Mice were allowed to acclimate to the environment for at least 5 days before being used for experiments.

Sepsis was induced in mice by cecal ligation and puncture (CLP) as described previously (51). In brief, mice were anesthetized with 2% isoflurane inhalation. The abdomen was shaved and disinfected using povidone-iodine. A 1.5-cm midline incision was made and the cecum was exposed, and ligated with 4-0 silk suture 1 cm proximal from the distal cecal tip. The cecum was punctured twice with a 22-guage needle and a small amount of feces was extruded. The cecum then was returned to the abdominal cavity and the wound was closed in layers. Sham mice underwent laparotomy only. Both sham and sepsis mice received a subcutaneous injection of antibiotic Imipenem at a dose 0.5 mg/mouse in 500 µL of normal saline and 500 µL of normal saline as resuscitation.

Analgesics and sedatives to mitigate pain and discomforts in septic mice have direct impacts on modulating immune responses in sepsis (52). In the current study to elucidate eCIRP's role in immune tolerance we avoided treating the animals with analgesics, and sedatives. We only used male mice because of the findings of previous studies indicating sex-specific differences in sepsis (53). It has been reported that male and female sex steroids exhibit diverse immune-modulating functions under normal conditions and varied disease processes (53). Experimental studies in mice revealed a significantly increased survival rate of female mice following polymicrobial sepsis induced by CLP compared with male animals (54). Therefore, the immuno-neuroendocrine system that varies between male and female sex may not be ignored while making CLP model in animals to study sepsis pathogenesis.

In vivo administration of rmCIRP

Recombinant murine (rm) CIRP was prepared in-house and the quality control assays were performed as described previously (27). The quality of the purified protein was assessed by ponseu staining of the gel and/or western blotting. Functional assay of the protein was done by assessing the TNFα levels in the macrophages after treating them with purified rmCIRP. The level of LPS in the purified protein was measured by a limulus amebocyte lysate (LAL) assay (Cambrex, East Rutherford, New Jersey). Only the purified protein lots that were endotoxin free were considered for in vitro and in vivo experiments. We performed these quality control assays for each purified protein lot. To rule out a contribution from LPS in the inflammatory response to rmCIRP, our previous study showed that incubation with polymyxin B, an LPS-binding antibiotic, did not interfere with rmCIRP-induced production of TNF-α, whereas heat treatment reduced the activity of rmCIRP in macrophages (27). rmCIRP at a dose of 5 mg/kg BW or normal saline was administered into mice by intraperitoneal injection (*i.p.*). At 24 h after rmCIRP injection, mice were anesthetized and peritoneal lavage was collected for macrophages isolation and analyses.

Isolation of peritoneal macrophages, splenocytes and cell culture

Murine peritoneal macrophages and splenocytes were isolated from healthy adult mice. Mice were anesthetized with 2% isoflurane inhalation. Peritoneal cells were isolated by washing with cold Hank's Balanced Salt Solution (HBSS) without Ca^{++} an Mg^{++}, with 5% FBS. Collected peritoneal cells were washed once with cold HBSS by centrifugation at 300 × g for 10 min at 4^{o}C followed by using 0.5 ml RBC lysing buffer (BD Biosciences, San Jose, CA) for 5 min at room

temperature to lyse red blood cells (RBC). Peritoneal cells were cultured in RPMI 1640 medium supplemented with 10% heat-inactivated fetal bovine serum (FBS), 2 mM glutamine, 100 IU/ml penicillin-streptomycin and 25 mM HEPES (complete RPMI). Peritoneal macrophages were then allowed to adhere in the culture plates for 3 h at 37 ^{o}C in 5% CO_2. Non-adherent cells were removed by washing with culture medium. Adhered peritoneal macrophages were then detached from the plate using a cell scraper and counted. Isolated primary cells were cultured overnight prior to use.

Spleens were collected from the mice and passed through a 70 µm nylon cell strainer using the plunger end of a 5-ml syringe. The splenocyte suspension was centrifuged at 300 × g for 5 min at 4 °C. The cell pellet was suspended in 1 ml RBC lysing buffer (BD Biosciences) to lyse the RBC in the suspension followed by the wash of the cell with PBS. The cell pellets were then re-suspended into complete RPMI medium and counted the cells.

Mouse macrophage RAW264.7 cells were obtained from American Type Culture Collection (ATCC; Manassas, VA) and cultured in Dulbecco's Eagle's Medium (DMEM) containing 10% FBS, 2 mM glutamine, 100 IU/ml penicillin-streptomycin. The cells were cultured at 37^{o}C in 5% CO_2.

Enzyme-linked immunosorbent assay (ELISA)

Serum levels of eCIRP were determined by using an ELISA kit from Lifespan Biosciences (Seattle, WA). Cytokine levels of cell culture supernatants were analyzed by ELISA using the kits of tumor necrosis factor-α (TNF-α) and IL-6 from BD Biosciences (San Jose, CA), following the protocols described by the manufacturer.

Flow cytometry

To analyze the expression of IL-6R, CD206 on macrophages, isolated peritoneal macrophages, splenocytes or RAW264.7 macrophages were washed with PBS with 2% FBS (FACS buffer). To exclude any non-specific binding, we treated cells in FACS buffer with Fc receptor blocker (anti-mouse CD16/32, clone: 93; Biolegend) for 10 min, prior to staining the cells with fluorescent-labeled Abs and respective isotype control IgGs. A BD LSRFortessa flow cytometer (BD Biosciences) was used to perform the flow cytometry. For intracellular pSTAT3 staining, cells were fixed and permeabilized, followed by staining with anti-pSTAT3 Abs or isotype IgGs. At least 3×10^4 cells were collected and analyzed with flow Jo software (TreeStar, Ashland, OR). Unstained and single color stained cells were used for setting up compensation in the measurement.

Real-time quantitative reverse transcription-polymerase chain reaction (qRT-PCR)

Total RNA was extracted from RAW264.7 macrophages (ATCC) using Trizol reagent (Thermo Fisher). cDNA was synthesized using MLV reverse transcriptase (Thermo Fisher). PCR reactions were carried out in 25 µl of a final volume in SYBY Green master mix (Thermo Fisher) with 0.08 µm of each forward and reverse primers **(Supplemental Table 1)** and cDNA. Amplification was conducted in a Step One Plus real-time PCR machine (Thermo Fisher) and analyzed by the 2^{-ddCT} method for relative quantitation normalized to mouse β-actin mRNA expression. The relative expression of mRNA was expressed as fold change in comparison with un-treated control.

Western blotting

Cells were harvested and lysed in lysis buffer (10 mM Tris-HCL, pH 7.5, 100 mM NaCl, 1 mM EDTA, 1mM EGTA, 1% Triton-X 100) containing protease inhibitor and phosphatase inhibitor cocktail tablet (Thermo Fisher). Cell lysates were fractionated on 4-12% Bis-Tris gels and transferred to nitrocellulose membrane. After blocking with 0.1% casein in Tris buffered saline (TBST), the membranes were incubated in anti-mouse pSTAT3, STAT3, β-actin Abs overnight at 4^{o}C. The target bands were detected by using infrared dye labeled secondary Abs and Odyssey Clx image system (Li-Cor Biosciences). The intensities of the bands were analyzed using Image Studio Ver 5.2 software (Li-Cor Biosciences).

Detection of the binding of eCIRP and IL-6R by surface plasmon resonance

Surface plasmon resonance (SPR) technology was used to examine the interaction of eCIRP and IL-6R. SPR was conducted using BIAcore 3000 instrument (GE healthcare) to analyze the binding between recombinant human (rh) CIRP (Origene, Rockville, MD) and rhIL-6R (R&D System). According to the manufacturer, rhCIRP was produced with TrueORF clone, RC201639 and was expressed in human HEK293T cell line. The protein was tagged with C-Myc/DDK and recombinant protein was captured through anti-DDK affinity column followed by conventional chromatography steps. rhIL-6R was prepared in *Spodoptera frugiperda*, *Sf* 21 (baculovirus)-derived human IL-6R alpha protein Leu20-Asp358. rhIL-6R used in the BIAcore assay did not contain any tags. Endotoxin levels in the purified protein was assessed as <1.0 EU per 1 μg of the protein using the LAL method. The binding reaction was performed in 1 × PBS buffer containing 0.01% Tween-20 (pH 7.4). The CM5 dextran chip (flow cell-2) was first activated by injection with 89 μl of 0.1 M N-ethyl-N'-[3-diethylaminopropyl]-carbodiimide and 0.1 M N-hydroxysuccinimide. An aliquot of 200 μl of 5 μg/ml of the ligand (rhIL-6R) diluted in10 mM

sodium acetate (pH 4.5) was injected into flow cell-2 of the CM5 chip for immobilization. Then, 135 µl of 1 M ethanolamine (pH 8.2) was injected to block the remaining active sites. The flow cell-1 without coating with the ligand was used as a control to evaluate nonspecific binding. The binding analyses were performed at a flow rate of 30 µl/min at 25^{o}C. To evaluate the binding, the analyte rhCIRP, ranging from 0 µM (or PBS as vehicle control) to 1.0 µM for the kinetics analysis or 0.5 µM rhCIRP for the yes-or no binding analysis was injected into flow cell-1 and flow cell-2, and the association of analyte and ligand was recorded by SPR. The signal from the blank channel (flow cell-1) was subtracted from the channel coated with the ligand (flow cell-2). Data were analyzed by the BIAcore 3000 Evaluation software. For all samples, a blank injection with buffer alone was subtracted from the resulting reaction surface data. Data were globally fitted to the Langmuir model for 1:1 binding.

Detection of the binding of eCIRP and IL-6R by immunofluorescent staining and FRET

Peritoneal macrophages were treated with rmCIRP (5 µg/ml) for 10 min at 4^{o}C and then fixed immediately with 4% paraformaldehyde. After a brief rinse with PBS, the cells were incubated with an Ab mixture of anti-mouse CIRP (1:35) and anti-mouse IL-6R (1:30). The cells incubated in anti-mouse CIRP Ab (1:35) with anti-mouse CD11b Ab (1:50) served as a control for the co-localization of rmCIRP and IL-6R. Confocal microscopy images were obtained using a Zeiss LSM880 confocal microscope under 63 × objective (Zeiss, Oberkochen, Germany).

The interaction of eCIRP and IL-6R was further analyzed employing fluorescence resonance energy transfer (FRET) technology (55). Peritoneal macrophages in a 96-well plate were treated with rmCIRP for 10 min at 4 ^{o}C and fixed with 4% paraformaldehyde. Similar to the immunostaining above, after the wash, the cells were incubated in the Abs mixture of anti-

mouse CIRP with anti-mouse IL-6R or anti-mouse CIRP with anti-mouse CD11b. Cy3-labeled anti-rabbit IgG and Cy5 labeled anti-goat IgG were used as secondary Abs. When the fluorophores of a FRET donor and a FRET acceptor were in proximity with the proper orientation, FRET occurred between them shown as FRET units (55). The cell associated fluorecence was measured on a Biotek Synergy Neo2 (Biotek, VT) at 579 nm upon excitation at 540 nm (*E1*), at 681 nm after excitation at 640 nm (*E2*), and at 681 nm after excitation at 540 nm (*E3*). The transfer of fluorescence which is the binding status of the two molecules was calculated as FRET units using the formula: FRET unit = ($E3_{both}$ - $E3_{none}$) - [($E3_{cy5}$ - $E3_{none}$) x ($E2_{both}/E2_{cy5}$)] - [($E3_{cy3}$ - $E3_{none}$) x ($E1_{both}/ E1_{cy3}$)] (56).

Treatment of macrophages with recombinant mouse IL-6

RAW264.7 cells were treated with rmIL-6 (50 ng/ml) for 1 and 5 h. Total protein was extracted from each group and subjected to western blotting using pSTAT3, STAT3, and β-actin Abs. For the tolerance assay, RAW264.7 cells were first treated with rmIL-6 (50 ng/ml) for 20 h. After washing the cells with Opti-MEM medium (Life Technologies), cells were re-stimulated with LPS (10 ng/ml) for 5 h and TNF-α levels in the culture medium were assessed by ELISA.

Inhibition of IL-6Rα in macrophages by siRNA transfection

IL-6R siRNA, a pool of 3 target-specific 19-25 nt siRNA designed to abrogate IL-6Rα expression was purchased from Santa Cruz Biotechnology (catalog no.: sc-40065). A non-targeting 20-25 nt siRNA was used as control (catalog no.: sc-37007, Santa Cruz). Electroporation method was used for efficient transfection of IL-6R siRNA into RAW264.7 macrophages by using Neon Transfection System (catalog no.: MPK5000; Life Technologies,

Grand Island, NY). RAW264.7 cells were cultured for 1-2 days in DMEM supplemented with 10% FBS, 2 mM glutamine, 100 IU/ml penicillin-streptomycin until cells were 70-90% confluent. The Neon transfection system (Life Technologies) which is paired with Neon kit (Life Technologies) was used for transfection of IL-6R siRNA in RAW264.7 cells by following the protocol of RAW264.7 cell transfection from the manufacture. A mixture of 1×10^5 cells and 50 pmol of IL-6Rα siRNA/control siRNA was taken into a 10 µl Neon tip, and the pipette was installed into the Neon pipette station for electroporation. Electroporated cells were immediately transferred into a 24-well plate containing 500 µl/well complete DMEM medium without penicillin-streptomycin. The parameters for electroporation were pulse voltage: 1680 volts, pulse width: 20 microseconds, and pulse number was 1. After 72 h culture, IL-6R expression in RAW264.7 cells was determined by western blot analysis. In an additional group, 72 h after siRNA transfection, RAW264.7 cells were treated with rmCIRP (1µg/ml) for 24 h, and then stimulated with LPS (10 ng/ml) for 5 h. The release of TNF-α and IL-6 in the culture supernatants were measured by ELISA.

Statistical analysis

All data were expressed as mean ± SEM. One-way ANOVA and student-Newman-Keuls (SNK) test were performed to compare among multiple groups. All data were tested for normality. For comparison of two groups, we performed unpaired 2-tailed Student's *t* tests. A P value less than 0.05 was considered significant.

Study approval

All experiments were performed in accordance with the national Institutes of Health (NIH) guidelines for the use of experimental animals and were approved by the Institutional Animal

Care and Use Committee (IACUC) of the Feinstein Institute for Medical Research. The number of animals in each experiment was determined by using SigmaPlot 12.5 (Systat Software, Inc., San Jose, CA) and these predications were in line with our previous publication (51).

Author contributions

MZ, MA did experimental design. MZ, HTY performed animal works. MZ, GM, NLD performed in vitro experiments. MZ, NLD performed immunostaining and FRET studies. MZ, MA, PW analyzed the data. MA, MZ prepared the figures and wrote the manuscript. PW, NLD reviewed and edited the manuscript. PW conceived the idea and supervised the project.

Acknowledgements

This study was supported by the National Institutes of Health (NIH) grants R35GM118337 (P.W.) and R01GM129633 (M.A.). We thank Michael Bloch and Ying Zhang of University of Maryland and Archna Sharma of Center for Immunology and Inflammation (CII), Feinstein Institutes for Medical Research (FIMR) for BIAcore assays, Amanda Chen of microscopy core, FIMR for microscopic study, Mahendar Ochani of CII, FIMR for helping in animal surgery, Fangming Zhang of CII, FIMR for helping in some in vitro works, and Betsy Barnes, Center for Autoimmune, Musculoskeletal, and Hematopoietic Diseases, FIMR for the FRET assay help.

Competing financial and/or non-financial interests

One of the authors (PW) is an inventor of patent applications (WO/2010/120726 and 61/881.798) covering the fundamental concept of targeting CIRP for the treatment of inflammatory diseases,

licensed by TheraSource LLC. PW and MZ are co-founders of TheraSource LLC. Other authors declared that they have no competing interests.

References

1. Biswas SK, and Lopez-Collazo E. Endotoxin tolerance: new mechanisms, molecules and clinical significance. *Trends Immunol.* 2009;30(10):475-87.
2. Nomura F, Akashi S, Sakao Y, Sato S, Kawai T, Matsumoto M, et al. Cutting edge: endotoxin tolerance in mouse peritoneal macrophages correlates with down-regulation of surface toll-like receptor 4 expression. *J Immunol.* 2000;164(7):3476-9.
3. López-Collazo E, and del Fresno C. Pathophysiology of endotoxin tolerance: mechanisms and clinical consequences. *Crit Care.* 2013;17(6):242.
4. Vergadi E, Vaporidi K, and Tsatsanis C. Regulation of endotoxin tolerance and compensatory anti-inflammatory response syndrome by non-coding RNAs. *Front Immunol.* 2018;9:2705.
5. Foster SL, Hargreaves DC, and Medzhitov R. Gene-specific control of inflammation by TLR-induced chromatin modifications. *Nature.* 2007;447(7147):972-8.
6. El Gazzar M, Yoza BK, Chen X, Garcia BA, Young NL, and McCall CE. Chromatin-specific remodeling by HMGB1 and linker histone H1 silences proinflammatory genes during endotoxin tolerance. *Mol Cell Biol.* 2009;29(7):1959-71.
7. Mages J, Dietrich H, and Lang R. A genome-wide analysis of LPS tolerance in macrophages. *Immunobiology.* 2007;212(9-10):723-37.
8. Draisma A, Pickkers P, Bouw MP, and van der Hoeven JG. Development of endotoxin tolerance in humans in vivo. *Crit Care Med.* 2009;37(4):1261-7.
9. Medvedev AE, Lentschat A, Wahl LM, Golenbock DT, and Vogel SN. Dysregulation of LPS-induced Toll-like receptor 4-MyD88 complex formation and IL-1 receptor-associated kinase 1 activation in endotoxin-tolerant cells. *J Immunol.* 2002;169(9):5209-16.
10. Rajaiah R, Perkins DJ, Polumuri SK, Zhao A, Keegan AD, and Vogel SN. Dissociation of endotoxin tolerance and differentiation of alternatively activated macrophages. *J Immunol.* 2013;190(9):4763-72.

11. Lyroni K, Patsalos A, Daskalaki MG, Doxaki C, Soennichsen B, Helms M, et al. Epigenetic and transcriptional regulation of IRAK-M expression in macrophages. *J Immunol.* 2017;198(3):1297-307.
12. Brint EK, Xu D, Liu H, Dunne A, McKenzie AN, O'Neill LA, et al. ST2 is an inhibitor of interleukin 1 receptor and Toll-like receptor 4 signaling and maintains endotoxin tolerance. *Nat Immunol.* 2004;5(4):373-9.
13. Kinjyo I, Hanada T, Inagaki-Ohara K, Mori H, Aki D, Ohishi M, et al. SOCS1/JAB is a negative regulator of LPS-induced macrophage activation. *Immunity.* 2002;17(5):583-91.
14. Wang N, Liang H, and Zen K. Molecular mechanisms that influence the macrophage m1-m2 polarization balance. *Front Immunol.* 2014;5:614.
15. Porta C, Rimoldi M, Raes G, Brys L, Ghezzi P, Di Liberto D, et al. Tolerance and M2 (alternative) macrophage polarization are related processes orchestrated by p50 nuclear factor kappaB. *Proc Natl Acad Sci U S A.* 2009;106(35):14978-83.
16. Yin Z, Ma T, Lin Y, Lu X, Zhang C, Chen S, et al. IL-6/STAT3 pathway intermediates M1/M2 macrophage polarization during the development of hepatocellular carcinoma. *J Cell Biochem.* 2018;119(11):9419-32.
17. Hussain SF, Kong LY, Jordan J, Conrad C, Madden T, Fokt I, et al. A novel small molecule inhibitor of signal transducers and activators of transcription 3 reverses immune tolerance in malignant glioma patients. *Cancer Res.* 2007;67(20):9630-6.
18. Hunter CA, and Jones SA. IL-6 as a keystone cytokine in health and disease. *Nat Immunol.* 2015;16(5):448-57.
19. Braune J, Weyer U, Hobusch C, Mauer J, Brüning JC, Bechmann I, et al. IL-6 regulates M2 polarization and local proliferation of adipose tissue macrophages in obesity. *J Immunol.* 2017;198(7):2927-34.
20. Greenhill CJ, Rose-John S, Lissilaa R, Ferlin W, Ernst M, Hertzog PJ, et al. IL-6 trans-signaling modulates TLR4-dependent inflammatory responses via STAT3. *J Immunol.* 2011;186(2):1199-208.
21. Dobrovolskaia MA, Medvedev AE, Thomas KE, Cuesta N, Toshchakov V, Ren T, et al. Induction of in vitro reprogramming by Toll-like receptor (TLR)2 and TLR4 agonists in murine macrophages: effects of TLR "homotolerance" versus "heterotolerance" on NF-kappa B signaling pathway components. *J Immunol.* 2003;170(1):508-19.

22. Dalpke AH, Lehner MD, Hartung T, and Heeg K. Differential effects of CpG-DNA in Toll-like receptor-2/-4/-9 tolerance and cross-tolerance. *Immunology.* 2005;116(2):203-12.
23. Sato S, Nomura F, Kawai T, Takeuchi O, Mühlradt PF, Takeda K, et al. Synergy and cross-tolerance between toll-like receptor (TLR) 2- and TLR4-mediated signaling pathways. *J Immunol.* 2000;165(12):7096-101.
24. Aneja RK, Tsung A, Sjodin H, Gefter JV, Delude RL, Billiar TR, et al. Preconditioning with high mobility group box 1 (HMGB1) induces lipopolysaccharide (LPS) tolerance. *J Leukoc Biol.* 2008;84(5):1326-34.
25. Nishiyama H, Itoh K, Kaneko Y, Kishishita M, Yoshida O, and Fujita J. A glycine-rich RNA-binding protein mediating cold-inducible suppression of mammalian cell growth. *J Cell Biol.* 1997;137(4):899-908.
26. Aziz M, Brenner M, and Wang P. Extracellular CIRP (eCIRP) and inflammation. *J Leukoc Biol.* 2019;106(1):133-46.
27. Qiang X, Yang WL, Wu R, Zhou M, Jacob A, Dong W, et al. Cold-inducible RNA-binding protein (CIRP) triggers inflammatory responses in hemorrhagic shock and sepsis. *Nat Med.* 2013;19(11):1489-95.
28. Zhou Y, Dong H, Zhong Y, Huang J, Lv J, and Li J. The Cold-inducible RNA-binding protein (CIRP) level in peripheral blood predicts sepsis outcome. *PLoS One.* 2015;10(9):e0137721.
29. Yang H, Wang H, Levine YA, Gunasekaran MK, Wang Y, Addorisio M, et al. Identification of CD163 as an antiinflammatory receptor for HMGB1-haptoglobin complexes. *JCI Insight.* 2018;3(24).
30. Denning NL, Aziz M, Gurien SD, and Wang P. DAMPs and NETs in Sepsis. *Front Immunol.* 2019;10:2536.
31. Wang P, Ba ZF, Cioffi WG, Bland KI, and Chaudry IH. The pivotal role of adrenomedullin in producing hyperdynamic circulation during the early stage of sepsis. *Arch Surg.* 1998;133(12):1298-304.
32. Aziz M, Jacob A, Yang WL, Matsuda A, and Wang P. Current trends in inflammatory and immunomodulatory mediators in sepsis. *J Leukoc Biol.* 2013;93(3):329-42.

33. Wang P, and Chaudry IH. Mechanism of hepatocellular dysfunction during hyperdynamic sepsis. *Am J Physiol.* 1996;270(5 Pt 2):R927-38.
34. Cauvi DM, Song D, Vazquez DE, Hawisher D, Bermudez JA, Williams MR, et al. Period of irreversible therapeutic intervention during sepsis correlates with phase of innate immune dysfunction. *J Biol Chem.* 2012;287(24):19804-15.
35. Ward LD, Hammacher A, Howlett GJ, Matthews JM, Fabri L, Moritz RL, et al. Influence of interleukin-6 (IL-6) dimerization on formation of the high affinity hexameric IL-6.receptor complex. *J Biol Chem.* 1996;271(33):20138-44.
36. Rostam HM, Reynolds PM, Alexander MR, Gadegaard N, and Ghaemmaghami AM. Image based machine learning for identification of macrophage subsets. *Sci Rep.* 2017;7(1):3521.
37. Navegantes KC, de Souza Gomes R, Pereira PAT, Czaikoski PG, Azevedo CHM, and Monteiro MC. Immune modulation of some autoimmune diseases: the critical role of macrophages and neutrophils in the innate and adaptive immunity. *J Transl Med.* 2017;15(1):36.
38. Rackov G, Hernández-Jiménez E, Shokri R, Carmona-Rodríguez L, Mañes S, Álvarez-Mon M, et al. p21 mediates macrophage reprogramming through regulation of p50-p50 NF-κB and IFN-β. *J Clin Invest.* 2016;126(8):3089-103.
39. Takeda K, Clausen BE, Kaisho T, Tsujimura T, Terada N, Förster I, et al. Enhanced Th1 activity and development of chronic enterocolitis in mice devoid of Stat3 in macrophages and neutrophils. *Immunity.* 1999;10(1):39-49.
40. Melillo JA, Song L, Bhagat G, Blazquez AB, Plumlee CR, Lee C, et al. Dendritic cell (DC)-specific targeting reveals Stat3 as a negative regulator of DC function. *J Immunol.* 2010;184(5):2638-45.
41. Lang R, Patel D, Morris JJ, Rutschman RL, and Murray PJ. Shaping gene expression in activated and resting primary macrophages by IL-10. *J Immunol.* 2002;169(5):2253-63.
42. El Kasmi KC, Smith AM, Williams L, Neale G, Panopoulos AD, Panopolous A, et al. Cutting edge: A transcriptional repressor and corepressor induced by the STAT3-regulated anti-inflammatory signaling pathway. *J Immunol.* 2007;179(11):7215-9.
43. Makkouk A, and Weiner GJ. Cancer immunotherapy and breaking immune tolerance: new approaches to an old challenge. *Cancer Res.* 2015;75(1):5-10.

44. Cheng F, Wang HW, Cuenca A, Huang M, Ghansah T, Brayer J, et al. A critical role for Stat3 signaling in immune tolerance. *Immunity.* 2003;19(3):425-36.
45. Zeng Y, Kulkarni P, Inoue T, and Getzenberg RH. Down-regulating cold shock protein genes impairs cancer cell survival and enhances chemosensitivity. *J Cell Biochem.* 2009;107(1):179-88.
46. Guo X, Wu Y, and Hartley RS. Cold-inducible RNA-binding protein contributes to human antigen R and cyclin E1 deregulation in breast cancer. *Mol Carcinog.* 2010;49(2):130-40.
47. Lujan DA, Ochoa JL, and Hartley RS. Cold-inducible RNA binding protein in cancer and inflammation. *Wiley Interdiscip Rev RNA.* 2018;9(2).
48. Sakurai T, Yada N, Watanabe T, Arizumi T, Hagiwara S, Ueshima K, et al. Cold-inducible RNA-binding protein promotes the development of liver cancer. *Cancer Sci.* 2015;106(4):352-8.
49. Rawlings JS, Rosler KM, and Harrison DA. The JAK/STAT signaling pathway. *J Cell Sci.* 2004;117(Pt 8):1281-3.
50. van der Poll T, van de Veerdonk FL, Scicluna BP, and Netea MG. The immunopathology of sepsis and potential therapeutic targets. *Nat Rev Immunol.* 2017;17(7):407-20.
51. Aziz M, Yang WL, Matsuo S, Sharma A, Zhou M, and Wang P. Upregulation of GRAIL is associated with impaired CD4 T cell proliferation in sepsis. *J Immunol.* 2014;192(5):2305-14.
52. Peterson NC, Nunamaker EA, and Turner PV. To treat or not to treat: The effects of pain on experimental parameters. *Comp Med.* 2017;67(6):469-82.
53. Angele MK, Pratschke S, Hubbard WJ, and Chaudry IH. Gender differences in sepsis: cardiovascular and immunological aspects. *Virulence.* 2014;5(1):12-9.
54. Zellweger R, Wichmann MW, Ayala A, Stein S, DeMaso CM, and Chaudry IH. Females in proestrus state maintain splenic immune functions and tolerate sepsis better than males. *Crit Care Med.* 1997;25(1):106-10.
55. Okamoto K, and Sako Y. Recent advances in FRET for the study of protein interactions and dynamics. *Curr Opin Struct Biol.* 2017;46:16-23.

56. Doucey MA, Goffin L, Naeher D, Michielin O, Baumgärtner P, Guillaume P, et al. CD3 delta establishes a functional link between the T cell receptor and CD8. *J Biol Chem.* 2003;278(5):3257-64.

Figures and legends

Figure 1

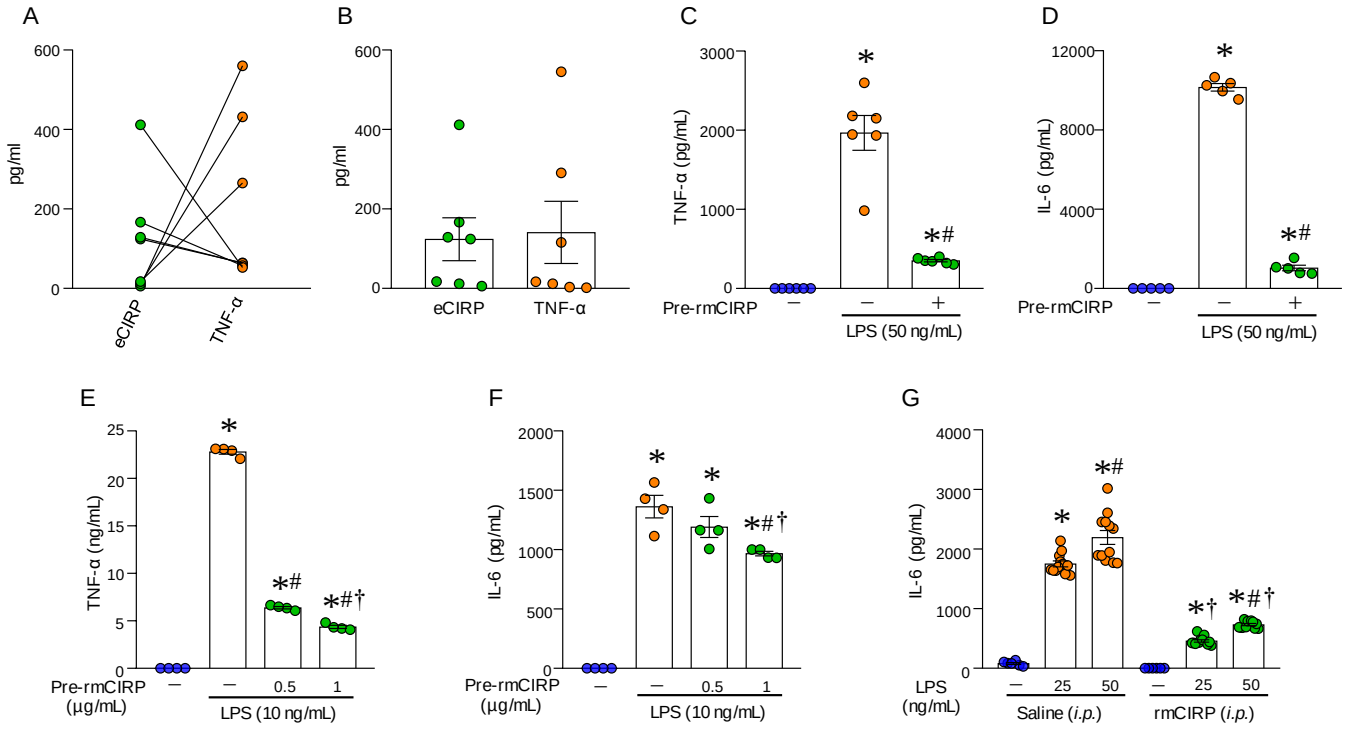

Figure 1. eCIRP induces macrophage tolerance. (A) Sepsis was induced in mice by CLP. 72 h after CLP, blood and spleen were collected. eCIRP levels in the serum was assessed. Splenocytes were isolated from the septic mouse and stimulated with LPS (100 ng/ml) for 5 h ex vivo and assessed for TNF-α in the culture supernatants. Data show the correlation between serum level of eCIRP and culture supernatant level of TNF-α from splenocytes treated with ex vivo LPS of each mouse. Green circle: eCIRP; orange circle: TNF-α. *n*=7 mice/group. **(B)** TNF-α levels in the serum was assessed and presented with serum levels of eCIRP. Data is expressed as mean ± SE

(n=7 mice/group). **(C, D)** A total of 7×10^5/ml peritoneal macrophages isolated from healthy mice were pre-stimulated with PBS or rmCIRP (1 μg/ml) for 24 h, and the cells were washed with medium. Macrophages were re-stimulated with LPS (50 ng/ml) for 5 h and assessed for **(C)** TNF-α and **(D)** IL-6 in the culture supernatants. Data is expressed as mean ± SE (n=5-6 wells/group). Experiments were repeated, and the repeated experimental data are shown in **Supplemental Figure 7**. $^*P < 0.05$ vs. PBS control, $^{\#}P < 0.05$ vs. pre-rmCIRP(-), LPS(+). **(E, F)** RAW264.7 macrophages (3×10^5/ml) were pre-treated with PBS or rmCIRP at 0.5 and 1.0 μg/ml for 24 h. Cells were washed with medium, re-stimulated with LPS (10 ng/ml) for 5 h and assessed for **(E)** TNF-α and **(F)** IL-6 in the culture supernatants. Data is expressed as mean ± SE (n=4 wells/group). Experiments were repeated, and the repeated experimental data are shown in **Supplemental Figure 7**. $^*P < 0.05$ vs. PBS control, $^{\#}P < 0.05$ vs. pre-rmCIRP(-), LPS(+), $^{\dagger}P < 0.05$ vs. rmCIRP (0.5 μg/ml). **(G)** Mice were injected with normal saline or rmCIRP (5 mg/kg BW) intraperitoneally *(i.p.)*. 24 h after injection, peritoneal macrophages were isolated. A total of 2×10^5 peritoneal macrophages were stimulated with 25 and 50 ng/ml LPS for 5 h ex vivo and assessed for IL-6 in the culture supernatants. Data is expressed as mean ± SE (n=6-12 samples/group). Experiments were performed two times, and all data were used for analysis. The groups were compared by one-way ANOVA and SNK method. $^*P < 0.05$ vs. PBS in respective injection group, $^{\#}P < 0.05$ vs. LPS (25 ng/ml) in respective injection group, and $^{\dagger}P < 0.05$ vs. saline injection in respective LPS dose. CLP, cecal ligation and puncture.

Figure 2

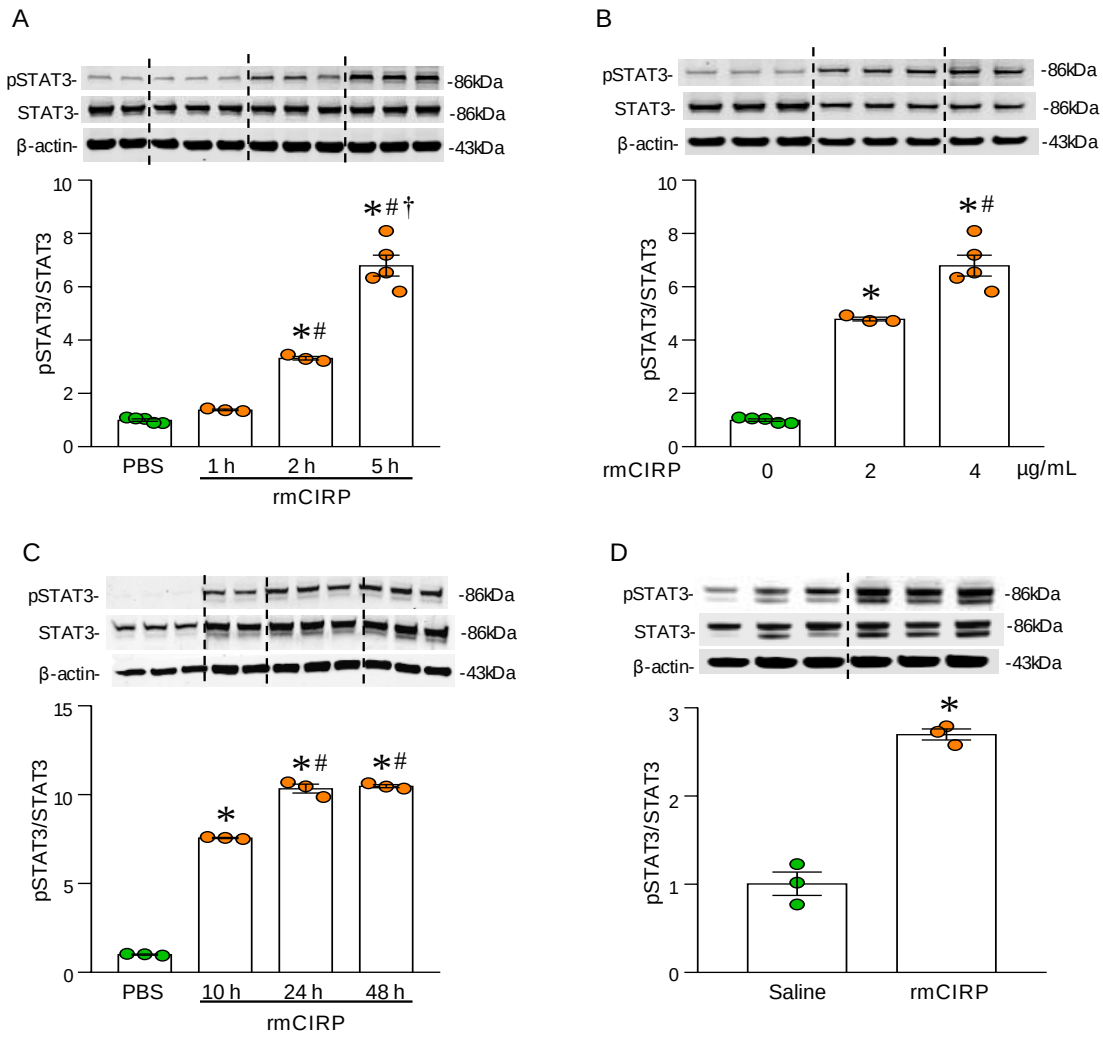

Figure 2. eCIRP induces STAT3 phosphorylation in macrophages. (A) RAW264.7 cells (8 × 10^5 cells/ml) were stimulated with rmCIRP (2 μg/ml) for 1, 2, and 5 h. Cells were harvested for protein extraction, followed by western blot using Abs against pSTAT3, STAT3, and β-actin. Data is expressed as mean ± SE (n=3-5 samples/group). Experiments were repeated, and the repeated experimental data are shown in **Supplemental Figure 8**. *$P < 0.05$ compared to PBS, $^{\#}P < 0.05$ compared to rmCIRP 1 h, $^{\dagger}P < 0.05$ compared to rmCIRP 2 h. **(B)** RAW264.7 cells (8 × 10^5 cells/ml) were stimulated with 2 and 4 μg/ml rmCIRP for 5 h. Cells were harvested for protein extraction, followed by western blot assays using Abs against pSTAT3, STAT3, and β–

actin. Data is expressed as mean ± SE (n=3-5 wells/group). Experiments were repeated, and the repeated experimental data are shown in **Supplemental Figure 8**. **P*<0.05 compared to PBS, #*P*<0.05 compared to rmCIRP (2 μg/ml). **(C)** Splenocytes isolated from healthy mice (2×10^6 cells/ml) were stimulated with rmCIRP (4 μg/ml) for 10, 24, and 48 h. Cells were harvested for protein extraction, followed by western blot using Abs against pSTAT3, STAT3, and β-actin. Data is expressed as mean ± SE (n=3 samples/group). Experiments were repeated, and the repeated experimental data are shown in **Supplemental Figure 8**. **P*<0.05 compared to PBS, #*P*<0.05 compared to rmCIRP 10 h. **(D)** Mice were injected with normal saline or rmCIRP (5 mg/kg BW) *i.p.*, after 24 h of PBS or rmCIRP injection, peritoneal macrophages were isolated for total protein extraction. Western blot was performed to determine pSTAT3, STAT3, and β-actin in each sample. Data is expressed as mean ± SE (n=3 mice/group). Experiments were repeated, and the repeated experimental data are shown in **Supplemental Figure 8**. **P* < 0.05 compared to saline injection. Representative western blots for pSTAT3, STAT3, and β-actin are shown. pSTAT3 expression in each sample was normalized to total STAT3 expression, and the mean values of PBS treated groups were standardized as one for comparison. Data is expressed as mean ± SE (n=3 samples/group). The groups were compared by one-way ANOVA and SNK method in multiple group comparisons. Two groups were compared by two-tailed Student's t test. STAT3, signal transducer and activator of transcription 3.

Figure 3

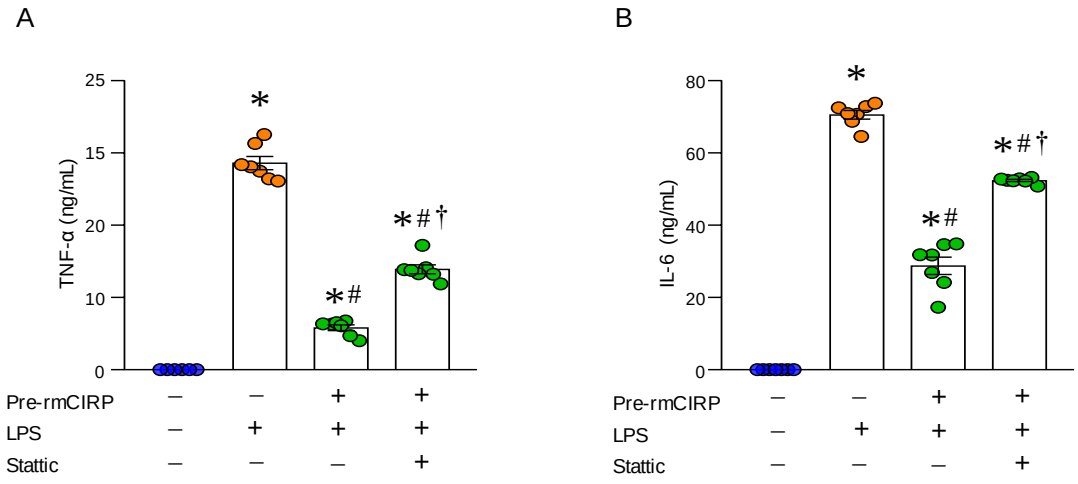

Figure 3. Inhibition of STAT3 by Stattic rescues macrophages from eCIRP-induced endotoxin tolerance. RAW264.7 cells (5×10^5/ml) were pre-treated with PBS or rmCIRP (1 µg/ml) in absence or presence of Stattic (3 µM) for 24 h. Cells were then washed with medium to remove supernatants and they were further stimulated with LPS (10 ng/ml). After 5 h, culture supernatants were collected and assessed for **(A)** TNF-α and **(B)** IL-6. Data is expressed as mean ± SE (n=7 samples/group). The experiments were performed three times, and all data were used for analysis. The groups were compared by one-way ANOVA and SNK method [*P<0.05 vs. pre-rmCIRP(-), LPS(-); #P<0.05 vs. pre-rmCIRP(-), LPS(+); †P<0.05 vs. pre-rmCIRP (+), LPS (+)]. rmCIRP, recombinant murine cold-inducible RNA-binding protein.

Figure 4

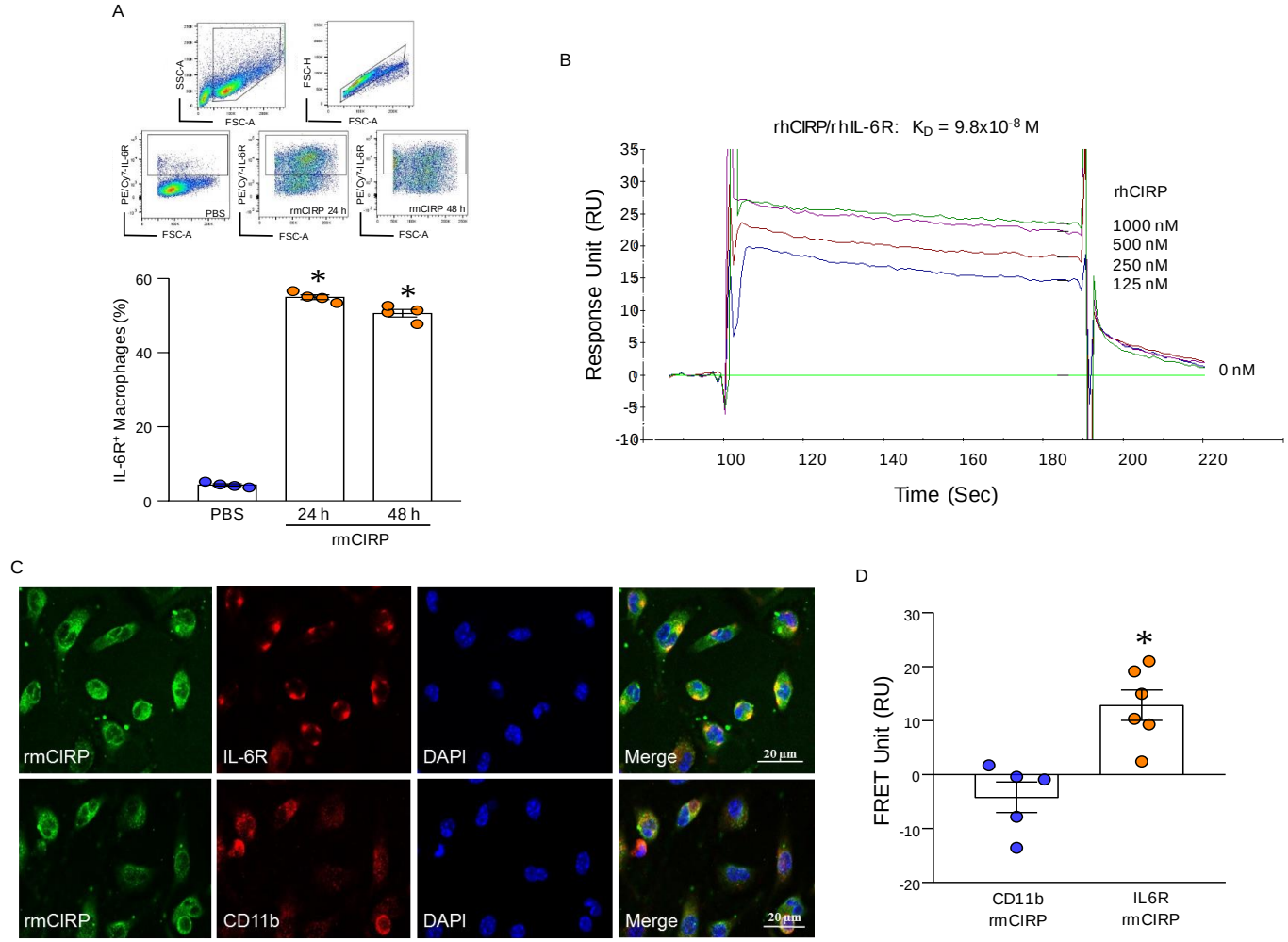

Figure 4. Identification of IL-6R as a novel receptor of eCIRP in macrophages. (A) RAW264.7 cells (1×10^6/ml) were stimulated with rmCIRP (1 μg/ml), and surface expression of IL-6R was assessed at 24 and 48 h following rmCIRP treatment by flow cytometry. Data is expressed as mean ± SE (n=4 samples/group). Experiments were repeated, and the repeated experimental data are shown in **Supplemental Figure 9**. The groups were compared by one-way ANOVA and SNK method (*P<0.05 vs. PBS). **(B)** SPR (Biacore assay) was performed between rhCIRP and rhIL-6R. rhIL-6R as ligand was immobilized on the chip. rhCIRP was injected as an analyte in concentrations of 0-1000 nM. The association and dissociation of analyte with ligand

at the indicated concentration were recorded and binding kinetics of rhCIRP and rhIL-6R was calculated. **(C)** Peritoneal macrophages (4×10^5/ml) were treated with rmCIPR (5 µg/ml) at 4ºC for 10 min and immediately fixed with paraformaldehyde, and stained with rabbit anti-mouse CIRP Ab, goat anti-mouse IL-6R Ab and goat anti-mouse CD11b Ab followed by Cy3-conjugated donkey anti-rabbit IgG and Cy5-conjugated donkey anti-goat IgG. The images were obtained by using a Zeiss confocal microscope under 63 x objective. The co-localization of rmCIRP and IL-6R is indicated by the merged images (yellow color). Scale bar 20 µM. (**D)** After the staining protocol described in **(C)**, cell associated fluorescence was measured on Biotek Synergy Neo2 at 579 nm upon excitation at 540 nm (*E1*), at 681 nm after excitation at 640 nm (*E2*) and at 681 nm after excitation at 540 nm (*E3*) for FRET unit calculation. The transfer of fluorescence was calculated as FRET units. FRET unit = $[E3_{both} - E3_{none}] - [(E3_{Cy5} - E3_{none}) \times (E2_{both}/E2_{Cy5})] - [(E3_{Cy3} - E3_{none}) \times (E1_{both}/E1_{Cy3})]$. Data is expressed as mean ± SE (n=5-6 wells/group). Experiments were repeated three times. Groups compared by two-tailed Student's t-test (*P<0.01 vs. CD11b). rmCIRP, recombinant mouse cold-inducible RNA-binding protein; FRET, fluorescence resonance energy transfer.

Figure 5

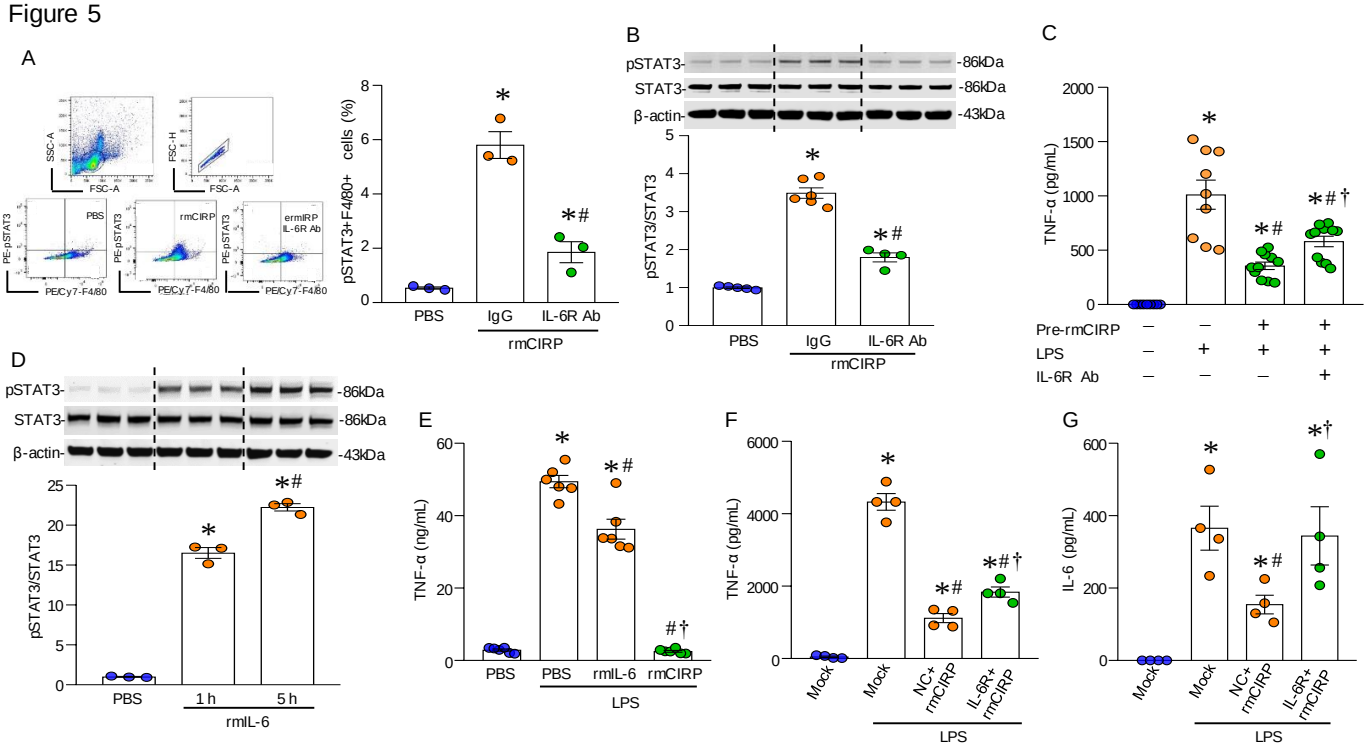

Figure 5. Inhibition of IL-6R corrects eCIRP-induced endotoxin tolerance. (A) Splenocytes were pre-treated with IgG or anti-IL-6R Ab and stimulated with rmCIRP for 5 h. Cells were fixed, permeabilized, and stained with anti-pSTAT3 and F4/80 Abs and analyzed. Data is expressed as mean ± SE (n=3 mice/group). The groups were compared by one-way ANOVA and SNK method (**P*<0.05 vs. PBS; #*P*<0.05 vs. IgG+rmCIRP). Experiments were repeated, and the repeated experimental data are shown in **Supplemental Figure 9**. **(B)** Peritoneal macrophages were pre-treated with IgG or anti-IL-6R Abs for 30 min, and stimulated with PBS or rmCIRP for 24 h. Total proteins were subjected to western blotting using anti-pSTAT3, STAT3, and β-actin Abs. Data is expressed as mean ± SE (n=4 samples/group). The groups were compared by one-way ANOVA and SNK method (**P*<0.05 vs. PBS; #*P*<0.05 vs. IgG + rmCIRP). Experiments were repeated, and the repeated experimental data are shown in **Supplemental Figure 10**. **(C)** Peritoneal macrophages were pre-treated with PBS or rmCIRP with IgG or anti-IL-6R Ab for 24

h. Cells were washed with medium and re-stimulated with LPS for 5 h. TNF-α levels in the supernatants were assessed. Data is expressed as mean ± SE (n=9-11 samples/group). Results were pooled from two independent experiments. The groups were compared by one-way ANOVA and SNK method [*P<0.05 vs. pre-rmCIRP(-), LPS(-); #P<0.05 vs. pre-rmCIRP(-), LPS(+); †P<0.05 vs. pre-rmCIRP (+), LPS (+)]. **(D)** RAW264.7 cells were treated with rmIL-6 for 1 and 5 h. Total protein was extracted and subjected to western blotting using pSTAT3, STAT3, and β-actin Abs. Data are expressed as means ± SE (n=3 samples/group). The groups were compared by one-way ANOVA and SNK method. *P < 0.05 compared to PBS-treated cells; $^{\#}P$ < 0.05 compared to rmIL-6 at 1 h. **(E)** RAW264.7 cells were treated with rmIL-6 for 20 h, and were re-stimulated with LPS for 5 h and TNF-α levels in the medium were assessed. Data are expressed as means ± SE (n=6 samples/group). The groups were compared by one-way ANOVA and SNK method. *P<0.05 vs. PBS(+), LPS(-); #P<0.05 vs. PBS(+), LPS(+); †P<0.05 vs. LPS (+), rmIL-6(+). **(F, G)** RAW264.7 cells were transfected with mock, IL-6R siRNA or NC siRNA and treated with rmCIRP for 20 h. Cells were re-stimulated with LPS for 5 h and **(F)** TNF-α and **(G)** IL-6 levels in the culture medium were assessed. Data is expressed as mean ± SE (n=4 samples/group). Experiments were performed twice, and all data were used for analysis. The groups were compared by one-way ANOVA and SNK method. *P<0.05 vs. Mock(+), LPS(-); #P<0.05 vs. Mock(+), rmCIRP(-), LPS(+); †P<0.05 vs. NC(+), rmCIRP(+), LPS(+).

Figure 6

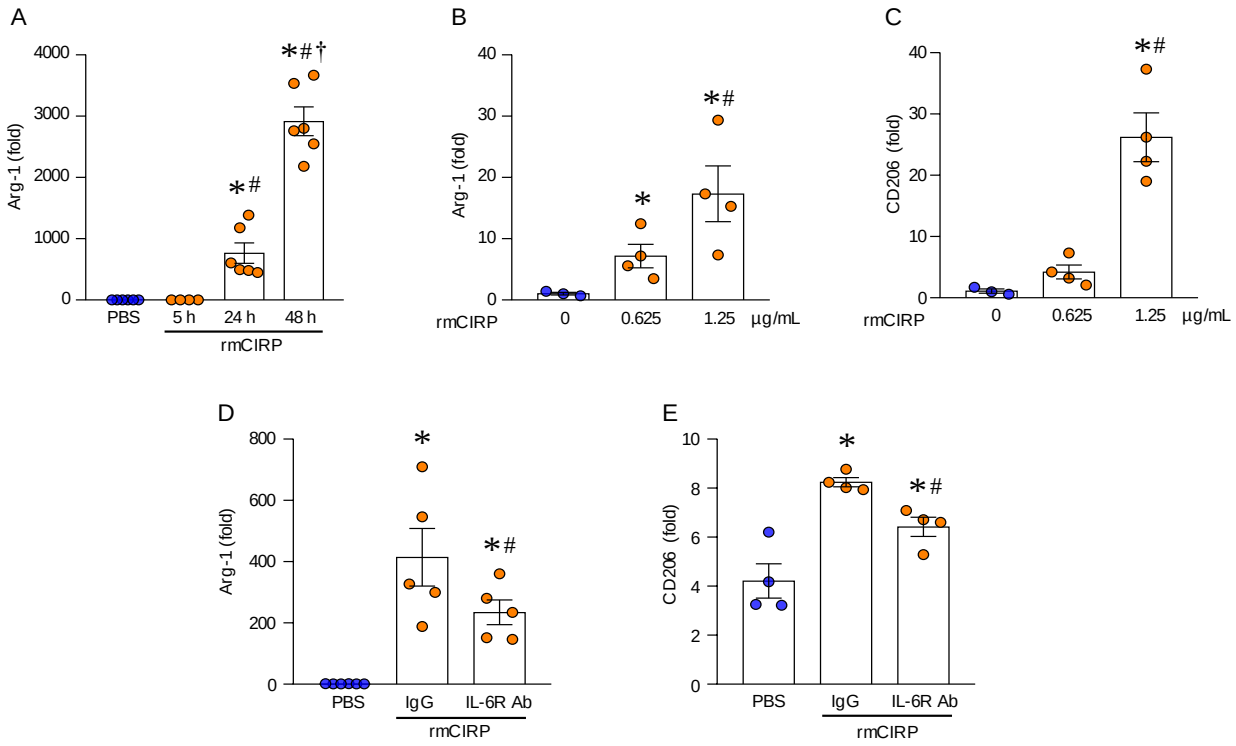

Figure 6. eCIRP induces M2 polarization through IL-6R. (A) RAW264.7 cells (1×10^6/ml) were treated with rmCIRP (1 μg/ml) for 5, 24, or 48 h. Arg-1 expression at mRNA levels were assessed by qPCR. Expression of Arg-1 was normalized to β-actin expression and represented as fold induction compared to the normalized values of PBS control-treated cells. Data is expressed as mean ± SE (n=4-6 samples/group). Experiments were repeated, and the repeated experimental data are shown in **Supplemental Figure 11**. The groups were compared by one-way ANOVA and SNK method [*P<0.05 vs. PBS (control); #P<0.05 vs. rmCIRP (5 h); †P<0.05 vs. rmCIRP (24 h). **(B, C)** RAW264.7 cells (1×10^6/ml) were treated with rmCIRP at dose of 0.625 and 1.25 μg/ml for 48 h, the expression of Arg-1 and CD206 mRNAs were assessed by qPCR and normalized to β-actin expression. Results are represented as fold induction compared to the normalized values of PBS control-treated cells. Data is expressed as mean ± SE (n=4

samples/group). Experiments were repeated, and the repeated experimental data are shown in **Supplemental Figure 11**. The groups were compared by one-way ANOVA and SNK method [*P<0.05 vs. rmCIRP (0 μg/ml); #P<0.05 vs. rmCIRP (0.625 μg/ml)]. **(D, E)** RAW264.7 cells (1 × 10^6/ml) were pre-treated with IgG (3 μg/ml) or anti-IL-6R Ab (3 μg/ml) for 30 min. These cells were then stimulated with PBS or rmCIRP (1 μg/ml) for 24 h, and then Arg-1 and CD206 were assessed by qPCR and flow cytometry, respectively. Arg-1 mRNA was normalized to β–actin and data expressed in fold induction was compared to PBS-treated condition. Data is expressed as mean ± SE (n=4-6 samples/group). Experiments were repeated two times, and all data were used for analysis. The groups were compared by one-way ANOVA and SNK method (*P<0.05 vs. PBS; #P<0.05 vs. IgG + rmCIRP).

Figure 7

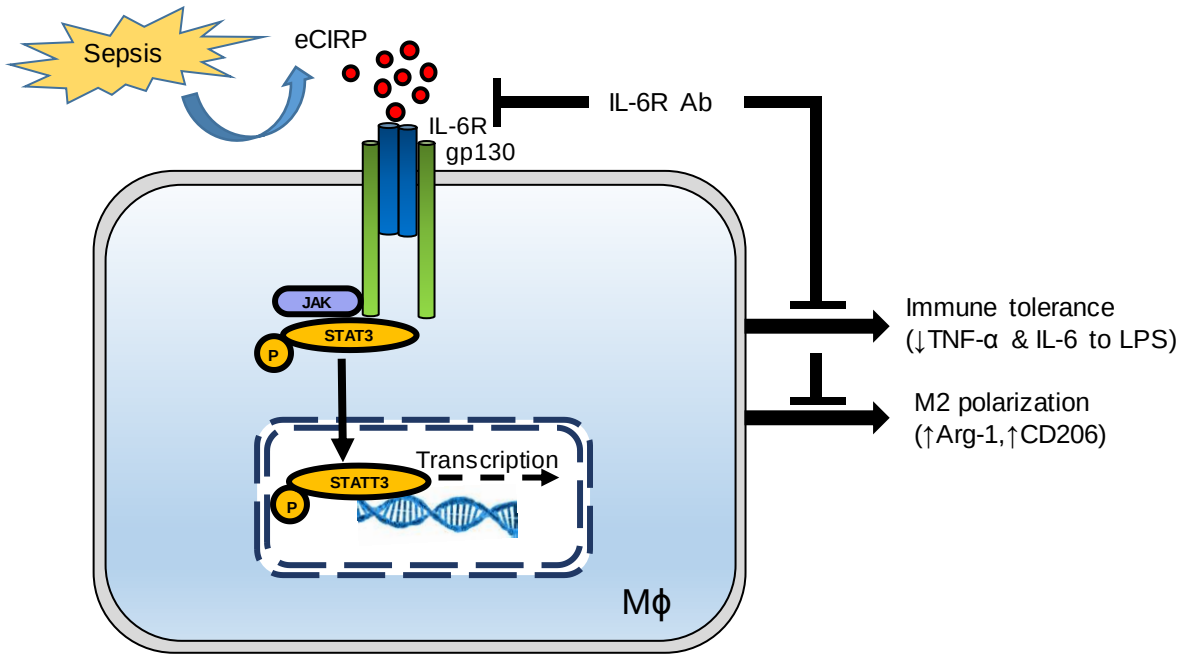

Figure 7. Hypothesis schema. eCIRP promotes macrophage endotoxin tolerance. eCIRP is increased during sepsis or other disease conditions and recognizes its novel receptor IL-6R

expressed in macrophages. This leads to the activation of down-stream transcription factor STAT3, which results in immune tolerance as depicted by decreased levels of TNF-α and IL-6 following LPS stimulation to these macrophages. eCIRP treatment of macrophages also induces regulatory phenotype M2 polarization in macrophages through IL-6R-dependent STAT3 activation. Inhibition of IL-6R by using its neutralizing Ab decreases eCIRP-induced STAT3 activation in macrophages and corrects immune tolerance and M2 polarization. STAT3, signal transducer and activator of transcription 3.